

Published in final edited form as:

*Pflugers Arch.* 2009 August ; 458(4): 777–783. doi:10.1007/s00424-009-0650-6.

## Silencing of ventromedial hypothalamic neurons by glucose-stimulated K<sup>+</sup> currents

Rhiannan H. Williams and Denis Burdakov

Department of Pharmacology, University of Cambridge, Tennis Court Road, Cambridge CB2 1PD, UK

### Abstract

Glucose sensing by neurons of the ventromedial hypothalamus (VMH) plays a central role in the regulation of body energy balance. Physiological rises in extracellular glucose levels hyperpolarise and inhibit a group of VMH neurons. This specialised sensing response is currently thought to involve glucose-induced activation of chloride channels, but alternative mechanisms have not been explored in detail. In this study, we converted all chloride channels from inhibitory to excitatory by filling the cytosol of VMH neurons with a high concentration of chloride. Despite this, some VMH neurons were still strongly hyperpolarised and inhibited by glucose. Voltage-clamp analysis revealed that this was due to glucose-induced activation of K<sup>+</sup>-selective currents of sufficient size to cause complete inhibition of whole-cell electrical activity. These K<sup>+</sup> currents exhibited leak-like biophysical properties and were inhibited by extracellular acidification. Our data support the idea that glucose-stimulated K<sup>+</sup> currents contribute to sugar-induced suppression of firing in the VMH.

### Keywords

Glucose; Feeding; Hypothalamus; Mouse; Electrophysiology

### Introduction

Healthy body weight in mammals depends on brain sensing of body energy resources; malfunction of this process leads to obesity [14, 25]. Glucose acts as a direct signal informing the brain about body energy status, and it has long been known that neurons of the ventromedial hypothalamus (VMH) specifically respond to changes in ambient glucose levels with changes in their firing rate [1]. These responses are thought to be critical for normal energy balance and glucose homeostasis [17, 23, 28]. It is thus important to elucidate the full mechanisms of how glucose alters the action potential firing of VMH cells.

Currently, there are two dominant theories of glucose sensing in the VMH, one explaining glucose-induced excitation and the other accounting for glucose-induced inhibition. Glucose-induced excitation of VMH neurons is thought to involve closure of K<sub>ATP</sub> channels [2, 18]. This theory has received substantial experimental support [21, 23, 27]. Importantly, however, some glucose-excited neurons remain functional in the VMH of K<sub>ATP</sub> channel

---

<sup>✉</sup> dib22@cam.ac.uk.

knockout mice, indicating an alternative,  $K_{ATP}$ -independent mechanism of glucose-induced excitation [11]. In turn, glucose-induced inhibition of VMH neurons has been proposed to involve opening of  $Cl^-$  channels [28, 31], but it has not been thoroughly explored whether other mechanisms can cause glucose-induced inhibition of firing in the VMH.

To determine whether glucose-induced hyperpolarisation in the VMH involves mechanisms other than  $Cl^-$  currents, in this study we analysed the electrical responses of VMH neurons to changes in extracellular glucose levels under conditions where  $Cl^-$ -induced inhibition was bio-physically impossible, using patch-clamp recordings in mouse brain slices.

## Materials and methods

### Preparation of brain slices

Procedures involving animals were carried out in accordance with the Animals (Scientific Procedures) Act, 1986 (UK). Mice (C57BL/6) were maintained on a 12-h light/dark cycle (lights on 0800 hours) and had free access to food and water. The animals were killed at 14–21 days postnatal during the day (the light phase), and coronal slices (250–300  $\mu$ m thick) containing the ventromedial hypothalamus were prepared as previously described [4]. Young animals were used for technical reasons (softer tissue greatly increases the chance of successful patch-clamp recordings) and to facilitate comparisons with previous electrophysiological studies of hypothalamic glucose sensing, which were performed using tissue from young animals (e.g., [23, 31, 32]). After slicing, brain tissue was kept at 35°C for 15 min and thereafter at room temperature until recording.

### Extracellular and intracellular solutions

For experiments involving changes in pH, we used a HEPES-buffered extracellular solution based on Hopwood and Trapp [16] to achieve greater pH control. This solution was bubbled with 100%  $O_2$  and contained (in mM): 118 NaCl, 3 KCl, 1  $MgCl_2$ , 1.5  $CaCl_2$ , 25 HEPES, 1 or 5 glucose, pH adjusted with NaOH. In all other experiments, we used a bicarbonate-buffered extracellular solution, which contained (in mM): 125 NaCl, 3 KCl, 2  $MgCl_2$ , 2  $CaCl_2$ , 1.2  $NaH_2PO_4$ , 26  $NaHCO_3$ , 1 or 5 glucose. The small osmolarity changes resulting from changes in extracellular [glucose] in our experiments were either compensated with sucrose or left uncompensated; no difference was observed between the two conditions. Intracellular (pipette) solutions were based on K-chloride and contained (in mM): 130 KCl, 0.1 EGTA, 10 HEPES, 5  $K_2ATP$ , 1 NaCl, 2  $MgCl_2$ , pH=7.3 with KOH. Tetrodotoxin was obtained from Tocris Cookson (Avonmouth, UK). All other chemicals were from Sigma (Poole, Dorset, UK).

### Electrophysiology and data analysis

For patch-clamp recordings, living neurons were visualised in brain slices using an Olympus BX50WI upright microscope equipped with infrared gradient contrast optics. Whole-cell patch clamp recordings and switching between voltage- and current-clamp modes were performed using an EPC-9 amplifier (Heka, Lambrecht, Germany) at 35°C as previously described [33]. Patch pipettes were pulled from borosilicate glass and had tip resistances of 3–5 M $\Omega$  when filled with the “K-chloride” pipette solution. Series resistances were in the

range of 5–10 MΩ and were not compensated. Data were sampled and filtered using Pulse/Pulsefit software (Heka) and analysed with Pulsefit and Origin (Microcal, Northampton, MA, USA) software. To monitor membrane resistance together with changes in membrane potential (Figs. 1a, b, 2a), cells were injected every 20–50 s with a fixed-amplitude (10–50 pA, 1-s duration) square pulse of hyperpolarising current [33]. The amplitude of the resulting downward deflections in membrane potential is proportional to membrane resistance (Ohm's law: resistance = voltage divided by current), i.e., inversely proportional to membrane conductance (conductance = current divided by voltage = 1/resistance).

Current–voltage relationships (Figs. 2b, 2c, 4b) were obtained by performing voltage-clamp ramps from 0 to –140 mV at a rate of 0.1 mV/ms, which is sufficiently slow to allow leak-like K<sup>+</sup> currents to reach steady-state at each potential [22]. In Fig. 2c, the net current–voltage relationship was fitted with the Goldman–Hodgkin–Katz current equation [15] in the following form:

$$I = P_K z^2 \frac{VF^2}{RT} \frac{[K^+]_i - [K^+]_o \exp(-zFV/RT)}{1 - \exp(-zFV/RT)}$$

Here,  $I$  is current (pA),  $V$  is membrane potential (mV),  $z$  is the charge of a potassium ion (+1),  $[K^+]_i$  is the pipette K<sup>+</sup> concentration (mM),  $[K^+]_o$  is the ACSF K<sup>+</sup> concentration (mM),  $T$  is temperature (Kelvin) and  $R$  and  $F$  have their usual meanings [15].  $P_K$  (a constant reflecting the K<sup>+</sup> permeability of the membrane) was the only free parameter during fits. The value of  $P_K$  used to obtain the fit shown in Fig. 2c was 0.026. Values are presented as means ± SEM.

## Control experiments

Our experimental rationale is based on making Cl<sup>−</sup> currents excitatory by dialysing neurons with a solution containing high [Cl<sup>−</sup>] by means of the whole-cell configuration of the patch-clamp technique. This makes the inside of the pipette continuous with the cytosol, thereby ensuring rapid exchange of small molecules by diffusion. We performed the following control experiments to check if this happens effectively. First, we added the fluorescent dye Lucifer Yellow to the pipette. By observing the patching process under an epifluorescence microscope, we found that the VMH neurons and their dendrites become rapidly filled with the fluorescent pipette solution (neurons became brightly fluorescent within a few seconds, and fluorescence reached maximum brightness in under 3 min,  $n=10$  cells). Second, we looked at the Cl<sup>−</sup> currents mediated by GABA<sub>A</sub> receptors, as in our previous studies [20]. We pharmacologically isolated GABA<sub>A</sub>-mediated spontaneous postsynaptic currents (PSCs) by blocking glutamate inputs with DAP5 and CNQX (procedure described in detail in [20]). Under these conditions, at the holding potential of –60 mV, no spontaneous PSCs were visible in VMH neurons when we used a “low-chloride” pipette solution that sets  $E_{Cl}$  to –58 mV ( $n=10$  cells, >1 min recording from each cell, the low-chloride solution is described in [6]). However, when we switched to the “high-chloride” solution described above ( $E_{Cl}=0$  mV), we observed large ( $42 \pm 5$  pA,  $n=10$  cells) inward PSCs that were blocked by 20 μM bicuculline ( $n=10$  cells, >1 min recording from each cell). The bicuculline-sensitive (i.e., GABA<sub>A</sub>-mediated) PSCs remained inward at a holding potential of –40 mV ( $n=10$  cells).

This confirms that our “high-chloride” pipette solution effectively manipulates the driving force for  $\text{Cl}^-$  and makes  $\text{Cl}^-$  currents inward and excitatory at typical resting membrane potentials of VMH neurons.

## Results

### Glucose inhibits a group of VMH neurons when $\text{Cl}^-$ currents are made excitatory

To make  $\text{Cl}^-$ -mediated hyperpolarisation and inhibition biophysically impossible, we used a KCl-based intracellular solution in all our experiments (see “Materials and methods”). This solution sets the  $E_{\text{Cl}}$  to  $\sim 0$  mV, thereby making the currents through all chloride channels excitatory. The baseline concentration of glucose in the VMH has been measured to be around  $\sim 1$  mM, and the maximum physiological level of glucose in the brain is thought to be around 5 mM [9, 11, 30]. Switching between 1 and 5 mM extracellular glucose caused a pronounced hyperpolarisation and inhibition of a subset of VMH neurons (Fig. 1a,  $n=13$  out of 60 recorded cells). The membrane potential of glucose-inhibited cells was  $-42 \pm 2$  mV in 1 mM glucose and  $-63 \pm 3$  mV after 10 min after switching to 5 mM glucose ( $n=11$ ;  $p < 0.001$ ). Smaller elevations in extracellular [glucose], from 1 to 2.5 mM, were also effective, hyperpolarising the cells by an average of  $8 \pm 1$  mV ( $n=4$ ). The hyperpolarising response was associated with a decrease in membrane resistance, estimated from membrane potential responses to hyperpolarising current pulses (Fig. 1a). Membrane resistance fell by  $52 \pm 3\%$  in 5 mM glucose compared with control values in 1 mM glucose measured in the same cell ( $n=6$ ). The largest resistance decrease was from 900 to 300 M $\Omega$ , and the smallest was from 1,500 to 1,200 M $\Omega$  in 1 and 5 mM glucose, respectively.

We also observed glucose-induced excitation in 15 out of 60 VMH neurons (Fig. 1b). In these cells, glucose-induced depolarisation was associated with a reduction in membrane conductance that had a reversal potential of  $-98 \pm 3$  mV ( $n=4$ , data not shown), consistent with glucose-induced closure of  $\text{K}^+$  channels, such as  $\text{K}_{\text{ATP}}$ . This confirms that the classical glucose-sensing machinery in the VMH was not disrupted by our experimental solutions.

These results indicate that a group of VMH neurons is hyperpolarised and silenced by glucose despite the fact that their  $\text{Cl}^-$  channels are incapable of producing hyperpolarisation (Fig. 1a). We noticed that most of these cells were located on the ventromedial edge of the VMH (nine out of 13 cells, locations of four cells were not determined) and so focused on this region (Fig. 1c) in all subsequent experiments.

### Glucose-induced inhibition is due to postsynaptic $\text{K}^+$ currents

Glucose-induced hyperpolarisation and concomitant decrease in membrane resistance persisted when the cells were synaptically isolated with tetrodotoxin (Fig. 2a,  $n=4$  out of 10 cells, the other six cells did not respond to glucose). This indicates that glucose-induced inhibition is not due to changes in action-potential-driven synaptic inputs. In the presence of tetrodotoxin, the membrane potential was  $-41 \pm 2$  mV in 1 mM glucose and  $-65 \pm 5$  mV in 5 mM glucose ( $n=4$ ;  $p < 0.01$ ). We also observed that glucose-induced hyperpolarisation and inhibition persisted when synaptic transmission was blocked using a low  $\text{Ca}^{2+}$  (0.3 mM),

high  $Mg^{2+}$  (9 mM) extracellular solution ( $n=4$ , data not shown). This confirms that glucose acted postsynaptically.

The above data suggest that glucose acts directly on recorded VMH neurons to activate an inhibitory current that is not carried by  $Cl^-$ . Indeed, under our ionic conditions,  $K^+$  currents are the only currents that can cause hyperpolarisation of recorded cells (deduced from the Nernst equation). To examine this directly, we looked at membrane currents by performing voltage-clamp recordings, a type of analysis for which our KCl-based intracellular solution is particularly well suited since it minimises junction potential errors, which occur in the whole-cell mode even when the pipette tip potential is nulled before giga-seal formation [3]. We measured whole-cell currents by obtaining whole-cell current–voltage ( $I-V$ ) relationships using voltage-clamp ramps (see “Materials and methods”). The net glucose-induced current was isolated by subtracting currents recorded in 1 mM extracellular glucose from those subsequently recorded from the same cell in 5 mM glucose (Fig. 2b, c). The reversal potential ( $E$ ) of the net glucose-induced current (Fig. 2b, c) was  $-100\pm 1$  mV ( $n=5$  cells), which is indistinguishable from  $E_K$  in our solutions ( $-102$  mV). This confirms that the glucose-induced current in the cells we studied is highly selective for  $K^+$  ions and does not contain a detectable contribution from  $Cl^-$  currents, since the latter would shift the reversal potential to more positive values than  $E_K$  (because  $E_{Cl^-}\sim 0$  mV). The  $I-V$  relationship of the net glucose-activated current in VMH neurons showed a mild outward rectification that was well approximated by the Goldman–Hodgkin–Katz equation current equation (Fig. 2c). This is consistent with a background  $K^+$  conductance lacking intrinsic voltage dependence [15].

### Glucose-stimulated $K^+$ currents are sufficiently large to silence electrical activity and are found in different classes of VMH neurons

To test whether the glucose-induced  $K^+$  currents (mean magnitudes shown in Fig. 2c) were large enough to account for glucose-induced electrical silencing, we directly injected hyperpolarising currents of similar or smaller magnitudes into VMH neurons. This reproduced the inhibitory effects of glucose on the membrane potential and firing rate of VMH neurons that were previously identified as glucose-inhibited (Fig. 3a,  $n=5$  cells). This confirms that the observed glucose-stimulated  $K^+$  currents are large enough to cause significant membrane hyperpolarisation of VMH neurons in which they operate.

To gain more information about the type of VMH neurons that sense glucose through glucose-stimulated  $K^+$  channels, we looked at their intrinsic electrical properties. From an electrophysiological perspective, VMH neurons fall into three subtypes (A, B and C) based on post-inhibitory “rebound” of the membrane potential [24]. These differences in the membrane potential dynamics are caused by different voltage-gated currents, e.g., low-threshold  $Ca^{2+}$  current produce rebound depolarisation/excitation, whilst A-type  $K^+$  channels produce rebound hyperpolarisation/inhibition (e.g., see [4]). To determine the electrical signatures of glucose-inhibited VMH neurons, we injected them with 1-s-long hyperpolarising current pulses and examined the time course of their membrane potential immediately after the termination of these pulses (Fig. 3b). This revealed that neurons displaying glucose-stimulated  $K^+$  channels did not form an electrically uniform cell

population: Some cells ( $n=4$ ) displayed no rebound (“type-A” fingerprint; Fig. 3b, top), others ( $n=4$ ) showed rebound excitation (“type-B” fingerprint; Fig. 3b, middle), whilst others still ( $n=4$ ) exhibited rebound inhibition (“type-C” fingerprint; Fig. 3b, bottom).

### Glucose-induced inhibition is reversed by acidification

To further characterise the properties of glucose-induced inhibition in the VMH, we tested whether it is affected by extracellular acidification, since we recently found an interaction between acid and glucose sensing in glucose-inhibited cells in the lateral hypothalamus [6]. We found that acidifying extracellular pH from 7.3 to 6 reversed the inhibitory effects of glucose on the membrane potential and action potential firing of VMH neurons (Fig. 4,  $n=4$  cells), whereas the same acidification before increasing [glucose] had negligible effects on membrane potential or current ( $n=3$ ). To examine whether acidification affects similar or different membrane conductances as those influenced by glucose, we periodically interrupted our current-clamp recordings to take measurements of the membrane  $I-V$  relationship using voltage-clamp ramps (Fig. 4a, see “Materials and methods”). This revealed that the acid-inhibited current had a reversal potential similar to that previously activated by glucose (Fig. 4b,  $n=4$  cells). Furthermore, like the glucose-activated current, the acid-inhibited current exhibited leak-like rectification ( $n=4$ , data not shown). This suggests that the effects of glucose on both membrane potential and current are selectively suppressed by extracellular acidification, consistent with the possibility that acid-sensitive background  $K^+$  channel(s), mediate  $Cl^-$ -independent inhibition of VMH neurons by glucose.

### Discussion

In this study, we show that glucose-stimulated  $K^+$  currents are sufficient to account for glucose-induced inhibition of some neurons in the VMH, a key center in the control of appetite and body weight [25]. This is unexpected because it is currently thought that  $Cl^-$  channels are predominantly responsible for direct inhibition of VMH neurons by glucose [10, 28, 31]. Our results demonstrate that a large proportion of glucose-sensing VMH neurons are hyperpolarised and electrically silenced by glucose through activation of postsynaptic currents that are selective for  $K^+$  and have no significant  $Cl^-$  component. At the moment, the behavioural or metabolic significance of these cells is unknown, but they displayed a variety of biophysical signatures (Fig. 3b), which can be indicative of different neurochemical and/or functional identities [4, 7].

What is the molecular identity of glucose-stimulated  $K^+$  currents? In this study, their biophysical properties resembled background or leak channels, displaying GHK current-voltage rectification (Fig. 2c). In addition, their activity was suppressed by extracellular protons (Fig. 4b). A functionally similar glucose-stimulated  $K^+$  current is present in the arousal-promoting orexin neurons of the lateral hypothalamus [6]. The “leak-like” GHK rectification is a key feature of the tandem-pore (KCNK) family of  $K^+$  channels [12]. However, there are at least 15 KCNK genes, theoretically giving rise to >200 possible dimeric channels with few pharmacological tools to distinguish between them [19], which makes the full molecular identity of glucose-stimulated leak-like  $K^+$  channels very difficult to determine. It is also possible that more than one type of  $K^+$  channel is stimulated by



glucose in glucose-inhibited neurons. For example, the conductance of putative glucose-stimulated channels is estimated to be 40 pS in lateral hypothalamic orexin neurons [6], but 132 pS in basomedial hypothalamic neurons [29]. Further, in contrast to hypothalamic cells, glucose-stimulated  $K^+$  currents in cells of the carotid body are voltage-gated [26]. Ultimately, a definitive test of candidate glucose-stimulated channels would require reconstitution of the glucose response in heterologous models, which requires better overall information on the nature of possible glucose receptor(s) and intracellular signalling pathway(s) in glucose-inhibited cells [13].

What are the relative contributions of  $K^+$  v  $Cl^-$  currents to glucose-induced inhibition in the VMH? Under our experimental conditions, where the reversal potentials for  $K^+$  and  $Cl^-$  are distinctly separated (0 and  $-100$  mV, respectively), this can be inferred from the reversal potential of the net glucose-activated current (Fig. 2c). If this potential is closer to  $-100$  mV,  $K^+$  channels contribute more, and if it is closer to 0 mV, then  $Cl^-$  channels form a dominant proportion of the current. The fact that our observed value is indistinguishable from  $-100$  mV (Fig. 2c) implies that under our recording conditions, there was no detectable contribution from  $Cl^-$  channels. This contrasts with the studies by Song et al. [31], which reported the reversal potential of glucose-activated current to be about  $-50$  mV when theoretical  $E_{Cl}$  is  $-57$  mV. There are several possible reasons for this discrepancy. First, Song et al. [31] used obesity-resistant (DR) rats, whilst we used wild-type mice. It is possible that genetic predisposition to obesity alters the mechanisms of glucose sensing in the VMH, and indeed, careful recent studies by Routh et al. increasingly support this scenario (e.g., [8]). It would be desirable to test whether depending on the animal's responses to different diets, glucose-inhibited VMH neurons switch from one biophysical mechanism of glucose sensing to another. However, because of the absence of specific molecular markers for VMH glucose-inhibited cells, this is currently very difficult to test on the same population of cells. Second, it is possible that different populations of glucose-inhibited VMH neurons use different biophysical mechanisms to sense glucose. Again, this is difficult to address effectively at present because there are no known specific inhibitors of  $K^+$  currents described here, and the  $Cl^-$  channel inhibitor gemfibrozil, used as a tool to study the role of  $Cl^-$  channels in glucose-induced inhibition [10], is also non-specific (discussed in [5]).

In summary, our results show that glucose-stimulated  $K^+$  currents make an important contribution to glucose-induced inhibition of firing in both the VMH and the lateral hypothalamus [6]. This suggests that wakefulness and energy balance-regulating neurocircuits share similar energy-sensing strategies, pointing to a wider role for glucose-stimulated  $K^+$  channels in brain function than originally anticipated.

## Acknowledgements

This work was supported by the Biotechnology and Biological Sciences Research Council.

## References

1. Anand BK, Chhina GS, Sharma KN, Dua S, Singh B. Activity of single neurons in the hypothalamic feeding centers: effect of glucose. *Am J Physiol.* 1964; 207:1146–1154. [PubMed: 14237464]

2. Ashford ML, Boden PR, Treherne JM. Glucose-induced excitation of hypothalamic neurones is mediated by ATP-sensitive K<sup>+</sup> channels. *Pflugers Arch.* 1990; 415:479–483. [PubMed: 2315006]
3. Barry PH, Lynch JW. Liquid junction potentials and small cell effects in patch-clamp analysis. *J Membr Biol.* 1991; 121:101–117. [PubMed: 1715403]
4. Burdakov D, Ashcroft FM. Cholecystokinin tunes firing of an electrically distinct subset of arcuate nucleus neurons by activating A-type potassium channels. *J Neurosci.* 2002; 22:6380–6387. [PubMed: 12151516]
5. Burdakov D, Gonzalez JA. Physiological functions of glucose-inhibited neurones. *Acta Physiol (Oxf).* 2009; 195:71–78. [PubMed: 18983451]
6. Burdakov D, Jensen LT, Alexopoulos H, Williams RH, Fearon IM, O’Kelly I, Gerasimenko O, Fugger L, Verkhatsky A. Tandem-pore K<sup>+</sup> channels mediate inhibition of orexin neurons by glucose. *Neuron.* 2006; 50:711–722. [PubMed: 16731510]
7. Burdakov D, Liss B, Ashcroft FM. Orexin excites GABAergic neurons of the arcuate nucleus by activating the sodium-calcium exchanger. *J Neurosci.* 2003; 23:4951–4957. [PubMed: 12832517]
8. Canabal DD, Potian JG, Duran RG, McArdle JJ, Routh VH. Hyperglycemia impairs glucose and insulin regulation of nitric oxide production in glucose-inhibited neurons in the ventromedial hypothalamus. *Am J Physiol Regul Integr Comp Physiol.* 2007; 293:R592–600. [PubMed: 17537841]
9. de Vries MG, Arseneau LM, Lawson ME, Beverly JL. Extracellular glucose in rat ventromedial hypothalamus during acute and recurrent hypoglycemia. *Diabetes.* 2003; 52:2767–2773. [PubMed: 14578295]
10. Fioramonti X, Contie S, Song Z, Routh VH, Lorsignol A, Penicaud L. Characterization of glucosensing neuron subpopulations in the arcuate nucleus: integration in neuro-peptide Y and pro-opio melanocortin networks? *Diabetes.* 2007; 56:1219–1227. [PubMed: 17261674]
11. Fioramonti X, Lorsignol A, Taupignon A, Penicaud L. A new ATP-sensitive K<sup>+</sup> channel-independent mechanism is involved in glucose-excited neurons of mouse arcuate nucleus. *Diabetes.* 2004; 53:2767–2775. [PubMed: 15504956]
12. Goldstein SA, Bockenhauer D, O’Kelly I, Zilberberg N. Potassium leak channels and the KCNK family of two-P-domain subunits. *Nat Rev Neurosci.* 2001; 2:175–184. [PubMed: 11256078]
13. Gonzalez JA, Reimann F, Burdakov D. Dissociation between sensing and metabolism of glucose in sugar sensing neurones. *J Physiol.* 2009; 587:41–48. [PubMed: 18981030]
14. He W, Lam TK, Obici S, Rossetti L. Molecular disruption of hypothalamic nutrient sensing induces obesity. *Nat Neurosci.* 2006; 9:227–233. [PubMed: 16415870]
15. Hille, B. *Ion channels of excitable membranes.* Sinauer; Sunderland, MA: 2001.
16. Hopwood SE, Trapp S. TASK-like K<sup>+</sup> channels mediate effects of 5-HT and extracellular pH in rat dorsal vagal neurones in vitro. *J Physiol.* 2005; 568:145–154. [PubMed: 16020457]
17. Levin BE, Dunn-Meynell AA, Routh VH. Brain glucose sensing and body energy homeostasis: role in obesity and diabetes. *Am J Physiol.* 1999; 276:R1223–R1231. [PubMed: 10233011]
18. Liss B, Roeper J. Molecular physiology of neuronal K-ATP channels (review). *Mol Membr Biol.* 2001; 18:117–127. [PubMed: 11463204]
19. Lotshaw DP. Biophysical, pharmacological, and functional characteristics of cloned and native mammalian two-pore domain K<sup>+</sup> channels. *Cell Biochem Biophys.* 2007; 47:209–256. [PubMed: 17652773]
20. Ma X, Zubcevic L, Bruning JC, Ashcroft FM, Burdakov D. Electrical inhibition of identified anorexigenic POMC neurons by orexin/hypocretin. *J Neurosci.* 2007; 27:1529–1533. [PubMed: 17301161]
21. Marty N, Dallaporta M, Thorens B. Brain glucose sensing, counterregulation, and energy homeostasis. *Physiology (Bethesda).* 2007; 22:241–251. [PubMed: 17699877]
22. Meuth SG, Budde T, Kanyshkova T, Broicher T, Munsch T, Pape HC. Contribution of TWIK-related acid-sensitive K<sup>+</sup> channel 1 (TASK1) and TASK3 channels to the control of activity modes in thalamocortical neurons. *J Neurosci.* 2003; 23:6460–6469. [PubMed: 12878686]
23. Miki T, Liss B, Minami K, Shiuchi T, Saraya A, Kashima Y, Horiuchi M, Ashcroft F, Minokoshi Y, Roeper J, Seino S. ATP-sensitive K<sup>+</sup> channels in the hypothalamus are essential for the maintenance of glucose homeostasis. *Nat Neurosci.* 2001; 4:507–512. [PubMed: 11319559]



24. Minami T, Oomura Y, Sugimori M. Electrophysiological properties and glucose responsiveness of guinea-pig ventromedial hypothalamic neurones in vitro. *J Physiol.* 1986; 380:127–143. [PubMed: 3612561]
25. Morton GJ, Cummings DE, Baskin DG, Barsh GS, Schwartz MW. Central nervous system control of food intake and body weight. *Nature.* 2006; 443:289–295. [PubMed: 16988703]
26. Pardal R, Lopez-Barneo J. Low glucose-sensing cells in the carotid body. *Nat Neurosci.* 2002; 5:197–198. [PubMed: 11850631]
27. Parton LE, Ye CP, Coppari R, Enriori PJ, Choi B, Zhang CY, Xu C, Vianna CR, Balthasar N, Lee CE, Elmquist JK, et al. Glucose sensing by POMC neurons regulates glucose homeostasis and is impaired in obesity. *Nature.* 2007; 449:228–232. [PubMed: 17728716]
28. Routh VH. Glucose-sensing neurons: are they physiologically relevant? *Physiol Behav.* 2002; 76:403–413. [PubMed: 12117577]
29. Rowe IC, Treherne JM, Ashford ML. Activation by intracellular ATP of a potassium channel in neurones from rat basomedial hypothalamus. *J Physiol.* 1996; 490(Pt 1):97–113. [PubMed: 8745281]
30. Silver IA, Erecinska M. Extracellular glucose concentration in mammalian brain: continuous monitoring of changes during increased neuronal activity and upon limitation in oxygen supply in normo-, hypo-, and hyperglycemic animals. *J Neurosci.* 1994; 14:5068–5076. [PubMed: 8046468]
31. Song Z, Levin BE, McArdle JJ, Bakhos N, Routh VH. Convergence of pre- and postsynaptic influences on glucosensing neurons in the ventromedial hypothalamic nucleus. *Diabetes.* 2001; 50:2673–2681. [PubMed: 11723049]
32. Song Z, Routh VH. Differential effects of glucose and lactate on glucosensing neurons in the ventromedial hypothalamic nucleus. *Diabetes.* 2005; 54:15–22. [PubMed: 15616006]
33. Williams RH, Jensen LT, Verkhatsky A, Fugger L, Burdakov D. Control of hypothalamic orexin neurons by acid and CO<sub>2</sub>. *Proc Natl Acad Sci U S A.* 2007; 104:10685–10690. [PubMed: 17563364]

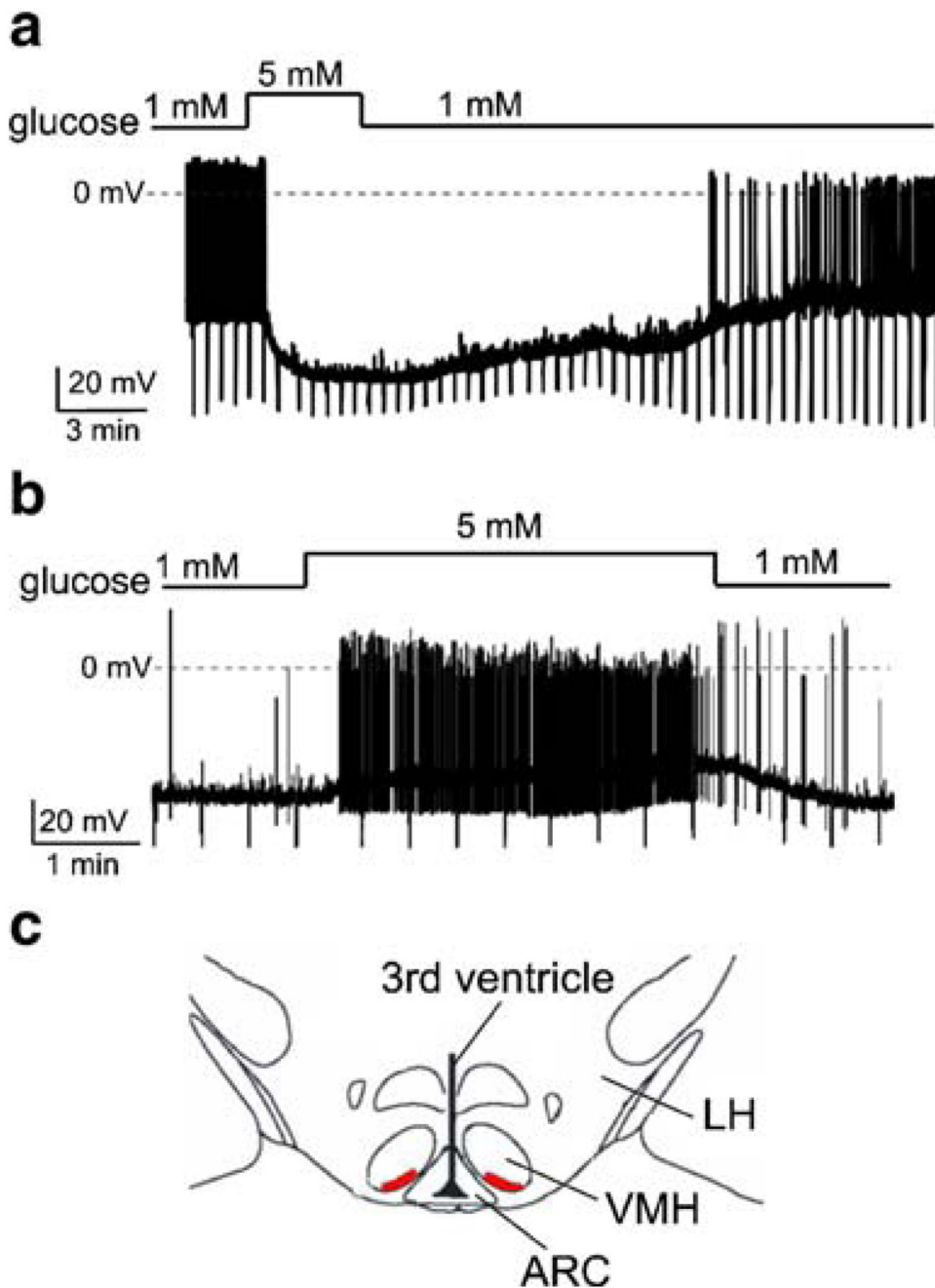


**Fig. 1.** Effects of glucose on the membrane potential of VMH neurons dialyzed with high  $[Cl^-]$ . Current-clamp whole-cell recordings. To monitor membrane resistance, cells were injected with periodic hyperpolarising current pulses (30 pA in **a** and 20 pA in **b**). The size of the resulting downward voltage deflections is proportional to membrane resistance. **a** Representative recording of an inhibitory response. Glucose causes hyperpolarisation, reduces membrane resistance and suppresses firing. **b** Representative recording of an excitatory response. Glucose causes depolarisation, increases membrane resistance and

increases firing. **c** Region of the VMH where we found glucose-inhibited neurons (*red*). *ARC* arcuate nucleus, *VMH* ventromedial hypothalamus, *LH* lateral hypothalamus. Slice shown approximately corresponds to adult mouse Bregma coordinates of  $-1.60$  to  $-1.85$  mm

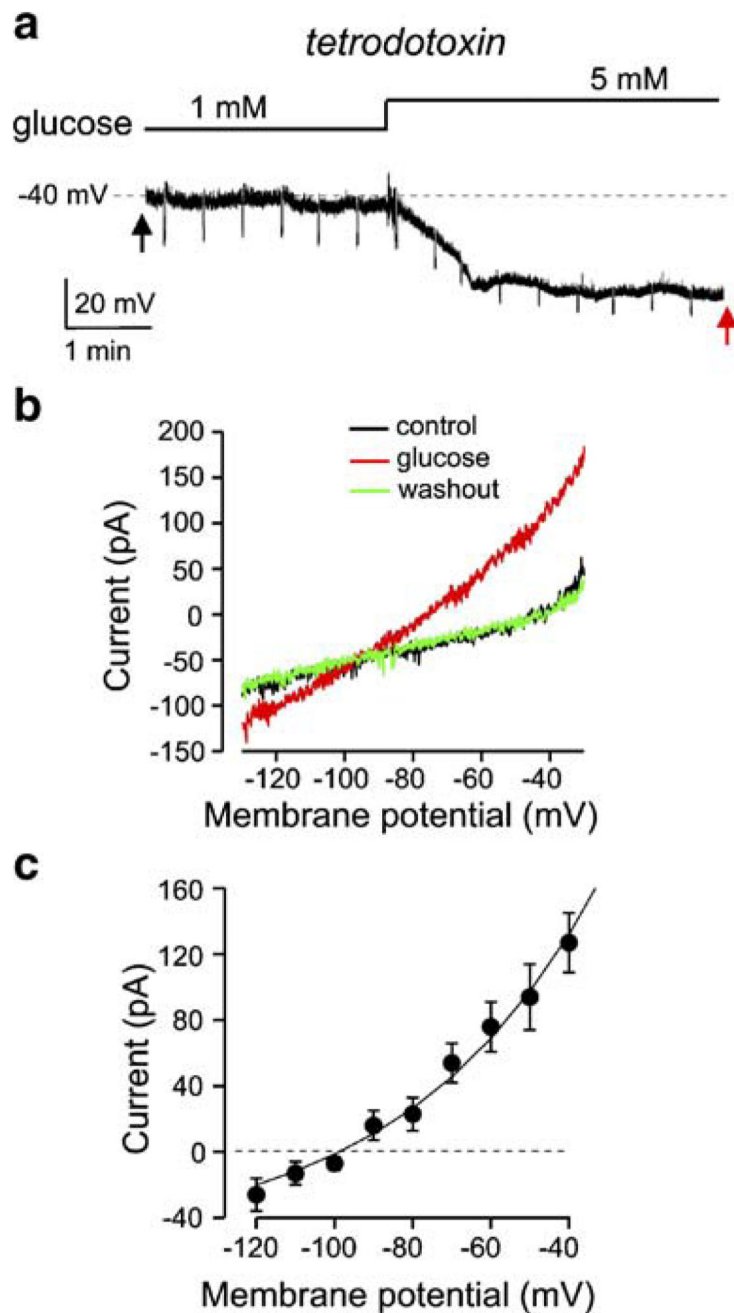


**Fig. 2.**

Postsynaptic currents underlying glucose-induced inhibition in the VMH. **a**. Glucose-induced hyperpolarisation and membrane resistance changes recorded in the presence of tetrodotoxin (1  $\mu$ M present in bath throughout the recording). Cell was periodically injected with 20 pA of hyperpolarising current to monitor membrane resistance. **b** Whole-cell voltage-clamp recordings of membrane  $I-V$  relationships of a glucose-inhibited neuron. **c**  $I-V$  plot of the net glucose-activated current. The line is a fit of the GHK equation to the data (see “Materials and methods”). Data are means  $\pm$  SEM ( $n=5$ )

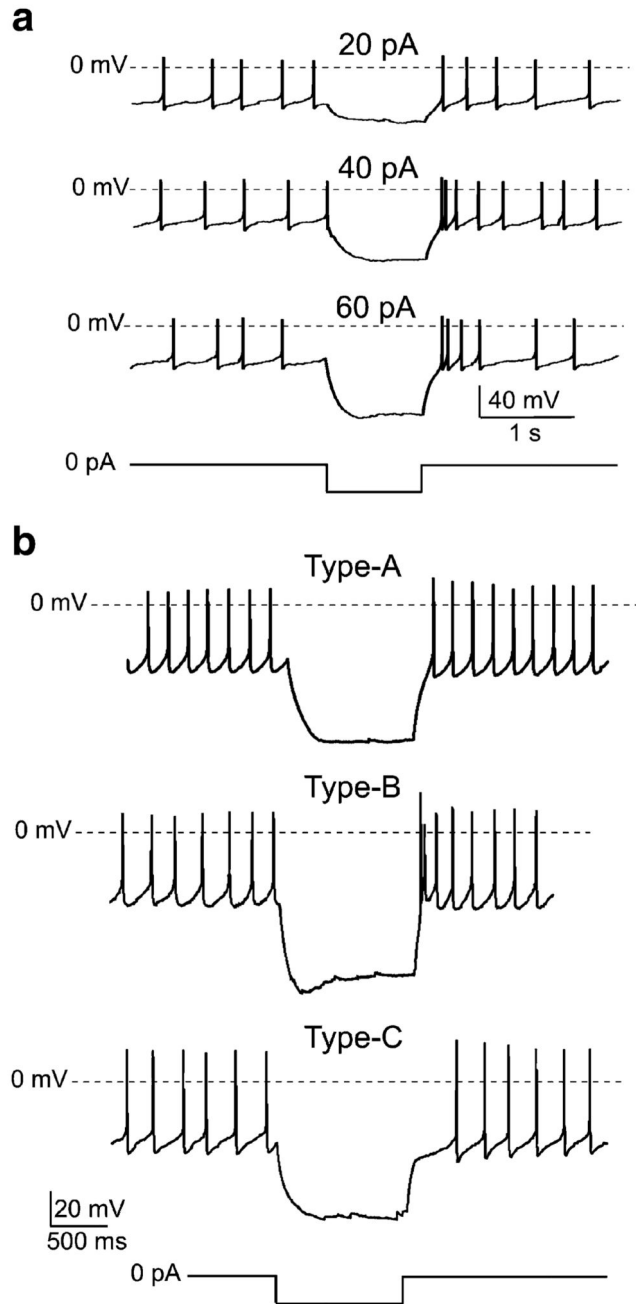


**Fig. 3.** Effects of current pulses on VMH neurons with glucose-stimulated  $K^+$  currents. **a** Effects of inhibitory current injections on a glucose-inhibited VMH cell. Current-clamp protocol is shown schematically below the traces. **b** Electrical fingerprints of glucose-inhibited VMH cells. The amplitude of the hyperpolarising current pulse was 50 pA

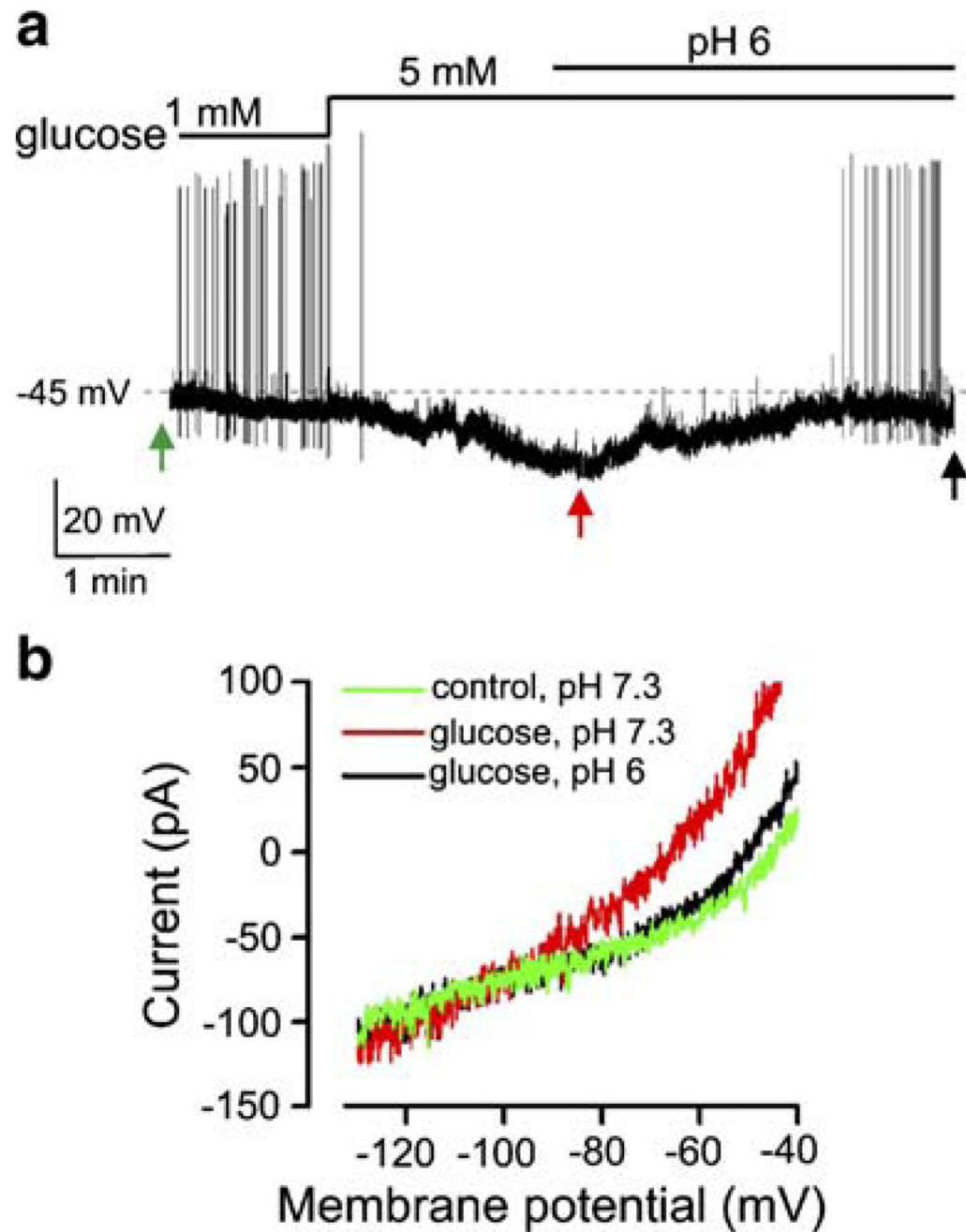


**Fig. 4.** Reversal of glucose-induced inhibition by extracellular acidification. **a** Effect of extracellular acidification on glucose-induced change in membrane potential of a VMH neuron. **b** Effect of extracellular acidification on glucose-induced change in membrane currents of the cell shown in **a**. *Arrows* correspond to the points where membrane ramps were taken